Nonlinear Model Predictive Control to reduce pitch actuation for floating offshore wind turbines

Saptarshi Sarkar, Breiffni Fitzgerald and Biswajit Basu

School of Engineering, Trinity College Dublin, Ireland, (e-mail: sarkars@tcd.ie, breiffni.fitzgerald@tcd.ie, basub@tcd.ie)

Abstract: Modern-day wind turbines use active pitch control to reduce mechanical loads on the turbines in addition to regulating generator power. These control algorithms increase blade pitch actuation, primarily to reduce the 1P (once per revolution) component of the aerodynamic load. However, it is also known that the failure of the blade pitch system is a significant source of turbine downtime. Control algorithms that increase pitch actuation will only add to this problem. Therefore, increasing blade pitch actuation to reduce mechanical loads may not be the best solution is every situation. Hence, in this paper, an individual pitch control strategy is proposed to reduce pitch actuation without deteriorating rotor speed regulation or increasing structural vibrations. The controller is developed under a Non-linear Model Predictive Control (NMPC) framework. It is assumed that a preview of the inflow wind field is available in the form of LIDAR (LIght Detection And Ranging) wind speed measurements. The results presented in this paper show that it is possible to reduce blade pitch actuation below the baseline level while maintaining rated rotor speed.

1. INTRODUCTION

The idea of reducing aerodynamic loads through individual blade pitch control (IPC) was put forward more than a decade ago by Bossanyi (2003, 2005). The success of the idea led to a significant amount of research conducted in successive years. Numerous individual blade pitch control strategies were presented by researchers all over the world. The industry has also accepted the use of these advanced control algorithms and modern wind turbines are now actively pitched to reduce mechanical loads. Field experiments were further conducted by Bossanyi et al. (2013) to validate the previously proposed IPCs.

Mughal and Guojie (2015) presented a discussion on various pitch control strategies from basic PID (proportional-derivative-integral) controllers to complex multivariable controllers like H_∞, neural network, adaptive control etc. The most prominent IPCs for floating offshore wind turbines were proposed by Namik and Stol (2010, 2011) based on a State Feeback Controller (SFC) and a Disturbance Accommodating Controller (DAC). In Namik and Stol (2014) the authors demonstrated the performance of the above two controllers on a spar-buoy floating wind turbine. The authors showed that while both controllers are capable of improving power regulation, the DAC has a detrimental effect on the platform motion. The SFC was inferior compared to the DAC in power regulation, but, the platform rolling and pitching rate was similar to that of the baseline controller. The authors recommended the use of the SFC since the platform motion was not amplified.

Model Predictive Control has gain popularity since the 1980s in industrial application and the same has been proposed for wind turbine control (Henriksen, 2011). LIDAR measurements can provide information about wind at various distances in front of the wind turbine. This information was used to design a nonlinear model predictive controller in (Schlipf et al., 2013). The controller was compared against the baseline controller and was shown to reduce extreme gust loads by 50% and lifetime fatigue loads by 30%. Some other prominent works on model predictive control for wind turbines are presented by (Odgaard et al., 2016; Soliman et al., 2010; Mirzaei et al., 2013). The model predictive control (MPC) framework has been used by Koerber and King (2013) to design wind turbine collective pitch and torque controller. The authors concluded that preview control provides significant benefits in normal operation and under gust conditions. In a first, a nonlinear model predictive controller for floating offshore wind turbines has been proposed in (Raach et al., 2014).

It may be noted here that the common characteristic of the IPCs reviewed above is that the control strategies aimed at reducing aerodynamic loads typically comes at the cost of increased pitch actuation. However, it is known (Valpy et al., 2017) that the blade bearings and pitch systems are a significant source of turbine downtime. Innovations that increase the load cycles on the pitch systems will only compound this problem. One way to reduce this downtime is innovations in improving bearing concepts and lubrication and improvements in hydraulic and electrical systems. However, with the current pitching systems, innovations in pitch control strategies that reduce pitch actuation offer

an alternative solution. Model predictive control has the potential of optimizing blade pitch actuation as it takes the future disturbance into account and the controller is optimal. This issue has not been investigated in the available literature and this paper aims to address this gap by proposing a new individual blade pitch control strategy that optimizes blade pitch actuation.

2. NON-LINEAR MODEL PREDICTIVE CONTROL OF BLADE PITCH ANGLES

A model predictive controller predicts the future behaviour of a system based on the current measurements, disturbance preview and an internal model. This basic concept of model predictive control is applicable to both linear and non-linear systems alike. In certain cases the system presents strong non-linearities that cannot be neglected (refer Schlipf et al. (2014)). In those situations non-linear model predictive control (NMPC) can significantly improve performance by considering the non-linearities of the system.

In this paper, the proposed NMPC controller assumes that a preview of the inflow wind field is available in the form of LIDAR (LIght Detection And Ranging) wind speed measurements. The details on the working of a LIDAR is not in the scope of this study and the interested reader may refer (Lindelöw, 2008) for details. A FAST-type 22-DOF spar-type Floating Offshore Wind Turbine (FOWT) model developed by the authors and benchmarked in Sarkar and Fitzgerald (2019) was augmented with linear uncoupled single degree of freedom pitch actuator models given by equation 1.

$$m_{\text{act}}\ddot{\beta}_i + c_{\text{act}}\dot{\beta}_i + k_{\text{act}}\beta_i = k_{\text{act}}\beta_i^c \qquad \text{for} \ \ i = 1 \text{ to } 3 \quad (1)$$

Where, $m_{\text{act}}, c_{\text{act}}$ and k_{act} are the actuator inertia, damping and stiffness terms respectively obtained from (Jonkman and Buhl Jr, 2005). The resulting dynamic model is a 25-DOF high-fidelity model of the floating wind turbine. The controller is developed using a simplified internal model and the performance of the controller is evaluated using the 25-DOF model.

2.1 Simplified reduced degree of freedom model

Model predictive control contains an internal model of the system embedded in the controller that is used to predict the future state of the system for a control sequence $\mathbf{u}(\cdot)$. For continuous time system the control system is obtained in the form

$$\dot{\mathbf{x}} = f(t, \mathbf{x}, \mathbf{u}) \quad (2)$$

For a complicated multi-degree of freedom systems, the internal model for the controller if often approximated by a reduced degree of freedom model Fitzgerald et al. (2018); Sarkar and Chakraborty (2018). In this paper, a nine degree of freedom reduced degree of freedom internal model presented in Appendix A is used to design the controller. The selected degrees of freedom are: the platform pitching degree of freedom (q_P), the tower fore-aft bending mode (q_T), the out-of-plane bending mode of the three blades (q_{Bi} for $i = 1, 2, 3$), the generator azimuth angle (q_{GeAz}) and the three blade pitch actuator motion (β_i for $i = 1, 2, 3$). The state vector can be given as

$$\mathbf{x} = [q_P, \ q_T, \ q_{B1}, \ q_{B2}, \ q_{B3}, \ q_{GeAz}, \ \beta_1, \ \beta_2, \ \beta_3]' \quad (3)$$
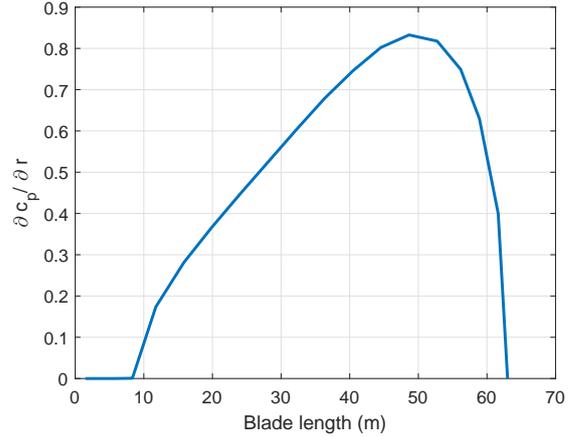

Fig. 1. Spanwise variation of power extraction

For details on the internal model please refer Sarkar et al. (2020).

2.2 Wind disturbance preview

The aerodynamic loads on the wind turbine is usually estimated using the Blade Element Momentum (BEM) theory. However, the internal model must be as simple as possible for implementation. For this purpose the aerodynamic loads on the wind turbine are estimated a-priori. The loads are obtained as a polynomial function of the effective wind speed (u_0) and blade pitch angles (β) by polynomial surface fitting of BEM results for various wind speeds and blade pitch angles. The reduced order model requires the information of the effective wind speed experienced by the blade in a way that encapsulates the information of the total wind field that the blade is subjected to. Hence, an effective wind speed at time t is defined as

$$u_0(t) = \sqrt[3]{\frac{\int_0^L u(t, r)^3 \frac{\partial c_p}{\partial r} r \mathrm{d}r}{\int_0^L \frac{\partial c_p}{\partial r} r \mathrm{d}r}} \quad (4)$$

where $\frac{\partial c_p}{\partial r}$ is the span-wise variation of power extraction factor obtained by modelling tip and hub losses following (Burton et al., 2011) shown in Figure 1. L is the length of the blade and r is the radial distance of the section under consideration from the root of the blade. Figure 2 shows the aerodynamic torque on the blades for different effective wind speeds and blade pitch angles. The forces and moments on the tower and platform are also estimated in the similar way.

2.3 Definition of the optimal control problem

The objective of the optimal control problem is to minimize a cost function J_{OCP} defined over a time horizon t_0 to T_f. The cost function is minimized by solving for an optimal control input trajectory $\mathbf{u}(\cdot)$ that minimizes the cost function in the presence of disturbance $\mathbf{d}(\cdot)$ subjected to a set of non-linear constraints that includes the dynamics of the internal model, the initial measurements and a set of non-linear constraints H that ensure feasible operational range. The optimization problem in continuous time can be described as
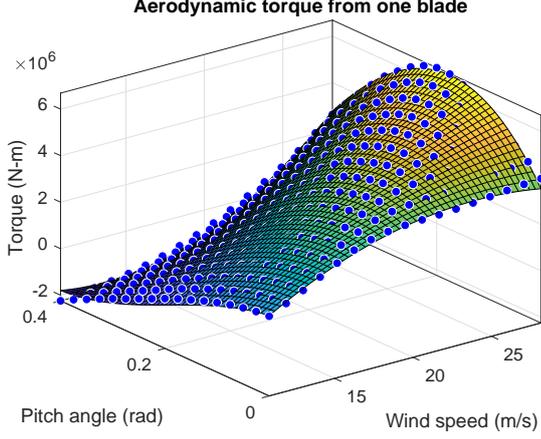
Aerodynamic torque from one blade

Fig. 2. Aerodynamic torque from blade

$$\min_{\mathbf{u}(\cdot)} J_{OCP}(\mathbf{x}, \mathbf{u}, \mathbf{d})$$

with: $\quad J_{OCP}(\mathbf{x}, \mathbf{u}, \mathbf{d}) = \int_{t_0}^{t_0+T_f} \Pi(\mathbf{x}(\tau), \mathbf{u}(\tau), \mathbf{d}(\tau)) \mathrm{d}\tau$

s.t. $\quad \dot{\mathbf{x}} = f(\mathbf{x}, \mathbf{u}, \mathbf{d})$

$\qquad \mathbf{x}(t_0) = \mathbf{x}_0$

$\qquad H(\mathbf{x}(\tau), \mathbf{u}(\tau), \mathbf{d}(\tau)) \geq 0 \quad \forall \tau \in [t_0, t_0 + T_f]$

$$\tag{5}$$

The primary aim of the present controller is to minimize blade pitch actuation while maintaining tracking of rated power at above rated wind speeds. The secondary objectives are to minimize platform pitching motion, the fore-aft bending of the tower and the flapwise bending of the blades. However, the aim of the controller is to achieve these goals at a reduced pitch actuation compared to the baseline controller. The objective function is defined as a quadratic function of system states multiplied with independent weights to emphasise on the different control objectives. The objective function is defined as

$$\Pi(\mathbf{x}(\tau), \mathbf{u}(\tau), \mathbf{d}(\tau)) = \quad Q_1(\dot{q}_{GeAz} - \Omega_{\text{rated}})^2 \tag{6}$$

$$+ Q_2(P(t) - P_{\text{rated}})^2 \tag{7}$$

$$+ Q_3\dot{q}_T^2 \tag{8}$$

$$+ Q_4\dot{q}_P^2 \tag{9}$$

$$+ [\dot{q}_{B1} \; \dot{q}_{B2} \; \dot{q}_{B3}]\mathbf{Q}_5[\dot{q}_{B1} \; \dot{q}_{B2} \; \dot{q}_{B3}]' \tag{10}$$

$$+ [\dot{\beta}_1 \; \dot{\beta}_2 \; \dot{\beta}_3]\mathbf{Q}_6[\dot{\beta}_1 \; \dot{\beta}_2 \; \dot{\beta}_3]' \tag{11}$$

In the above equation, Ω_{rated} and P_{rated} are the rated rotor speed and power output of the 5MW FOWT. The weights Q_1 and Q_2 penalises the rotor speed error and rated power error respectively. The velocity of tower fore-aft motion is penalised with Q_3 and the platform pitching velocity is penalised with the weight Q_4. $\mathbf{Q}_5$ and $\mathbf{Q}_6$ are diagonal matrices defined to penalise the blade flapwise velocity and blade pitch actuator velocities respectively.

Next, the set of constraints H that guarantees the feasible range of operation of the wind turbine is defined as

$$H := \begin{matrix} \beta_i^{\min} \leq \beta_i \leq \beta_i^{\max} \\ -\dot{\beta}_i^{\max} \leq \dot{\beta}_i \leq \dot{\beta}_i^{\max} \\ T_g^{\min} \leq T_g \leq T_g^{\max} \\ \dot{T}_g^{\max} \leq \dot{T}_g \leq \dot{T}_g^{\max} \end{matrix} \tag{12}$$
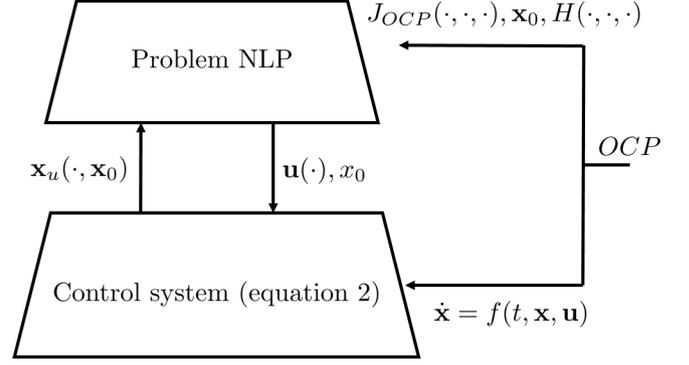

Fig. 3. Computation hierarchy and communication of data between elements

where, $\beta_i^{\min}$ and $\beta_i^{\max}$ and the minimum and maximum pitch angles respectively. $T_g^{\min}$ and $T_g^{\max}$ are the minimum and maximum allowable generator torque respectively. And $\dot{\beta}_i^{\max}$ and $\dot{T}_g^{\max}$ are the maximum allowable pitch and torque rate respectively.

The NMPC needs a preview of the blade effective wind speed over the prediction time T_f. In simulations, this is obtained easily from TurbSim (Jonkman, 2009) wind fields using equation 4. In reality, nacelle mounted LIDAR systems are capable of scanning the incoming wind field. It is possible to extract a rotor effective wind speed from the raw data delivered by such a LIDAR system. This procedure is out of scope of the current study and a description is presented in (Schlipf et al., 2013). MATLAB's constrained non-linear programming solver `fmincon` has been used here to solve the optimal control problem. Sequential Quadratic Programming algorithm has been used in `fmincon` to minimize the cost function in equation 5.

The prediction horizon is chosen to be $T_f = 12$s which is a proper assumption (refer (Schlipf et al., 2013)). The time steps in the NLP are set equal to $\Delta t_{NLP} = 1.2$s, which in 11 stages (N=1) covers a time horizon of 12s ([N-1]Δt_{NLP}). The LIDAR wind measurements are assumed to have an update rate of 0.5s. Hence, wind disturbance preview is available at every 0.5, 1, 1.5,..., 12s. The effective wind speed $u_0(t)$ at any intermediate time t is obtained from linear interpolation. Therefore, after every 0.5s the LIDAR measurements are updated and the NLP is solved with new measured state.

A sliding horizon type control strategy is used in this paper where the control input is estimated for the entire finite time horizon; the predicted control input from the first stage is returned to close the control loop and the rest is discarded. The NLP is solved again for the new finite horizon for the measured initial state and disturbance prediction. Recursive elimination method is used to solve the optimal control problem in equation 5. In this method, the problem is divided into two sub-problems and they are solve separately using specialized methods. The hierarchy and communication of the control problem is shown in Figure 3.

A practical challenge from an implementation point of view is that the control input obtained from NMPC is discrete in time. Since, the pitch actuator model is

stiff, applying the control inputs in their original discrete form can amplify actuator motion due to the transient effect arising from step jumps in commanded pitch angles. To avoid this problem two steps are taken. Firstly, the commanded pitch angles are obtained by interpolating between the inputs of two stages. Hence, a step change in control input is transformed into a linear change. And secondly, the control input is passed through a single-pole low-pass filter with exponential smoothing (Jonkman and Buhl Jr, 2005) to eliminate high frequency variations in the control input. The proof of closed loop stability of the non-linear constrained system solved by a model predictive controller is beyond the scope of this work.
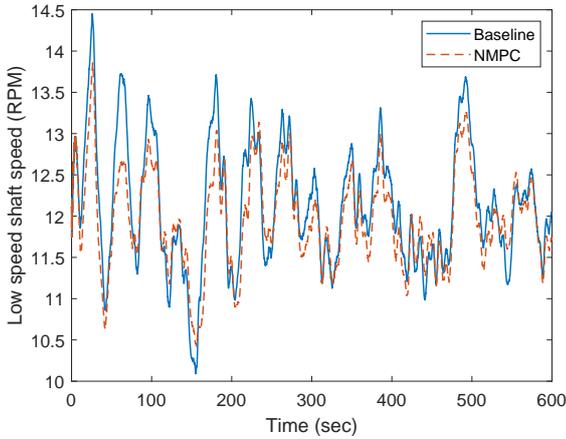
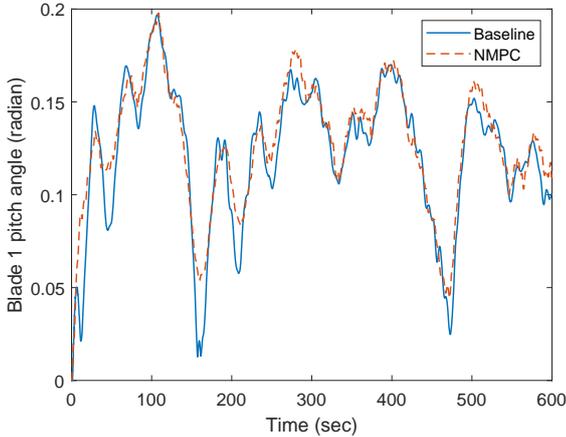## 3. RESULTS

Fig. 4. Low-speed-shaft speed

Fig. 5. Blade pitch angle

The performance of the controller is evaluated based on numerical time history analysis. The 5MW OC3 Hywind turbine, a spar-type FOWT, defined in (Jonkman, 2010) has been used for numerical purposes. MATLAB (2018) has been used as the simulation platform. A sampling rate of 40 Hz has been used for time integration using the runga-kutta 4th order method. The turbulent wind field is generated using the TurbSim (Jonkman, 2009) package. The stochastic sea is modelled by the Pierson-Moskowitz spectrum (Pierson Jr and Moskowitz, 1964). It

is important to note here that the pitch controller is active only in wind speed region 3 (above rated wind speed). Two load cases are chosen; Load Case 1: wind speed = 12.5 m/s, wave height 3 m and wave period 11 s, and, Load Case 2: wind speed = 14.5 m/s, wave height 3 m and wave period 11 s.

To conform with the length requirements of the paper, plot of the rotor speed and blade pitch angle are presented only for Load Case 2 in Figure 4 and Figure 5 respectively. The blade pitch angle is the most important parameter as the controller is designed to minimize blade pitch actuation or the variation of the blade pitch angles. The first thing to note is that the dynamics of the FOWT is not heavily altered by the NMPC controller compared to the baseline controller. This is because the blade pitch angle from the NMPC controller is not significantly different from the baseline controller as shown in Figure 5. It can be observed from the results that the baseline controller tracks the rated rotor speed with close to minimum blade pitch actuation. Therefore, the scope of further reduction of blade pitch actuation is limited. However, further scope of improvement arises from from the fact that unlike the baseline PI controller the NMPC controller provides an optimal control framework and the NMPC controller optimizes the control input based on information about the future. The controller also tracks the rated rotor speed with very good accuracy (see Figure 4), with reduced pitch actuation. To compare the two controllers quantitatively the standard deviations of the different FOWT responses are summarized in Table 1. It can be observed that the proposed IPC considerably reduces the platform pitching motion, the tower fore-aft motion and the blade out-of-plane motion as these degrees of freedom are included in the design of the controller. In the cross-wind direction, the platform rolling motion is slightly reduced. Other than that, the blade in-plane motion and tower side-to-side motion is left unaffected by the controller. The performance of the controller can be summarized by noting that the proposed NMPC controller is capable of improving the dynamic responses of the FOWT (rotor speed tracking and vibration control) with reduced pitch actuation compared to baseline controller.

4. CONCLUSION

In this paper an LIDAR-based individual blade pitch controller has been proposed to optimize blade pitch actuation. The results presented here can be concluded as follows

- The proposed IPC is capable of tracking the rated rotor speed with reduced pitch actuation compared to the baseline controller. The performance improves at higher wind speeds.
- At higher wind speeds the proposed IPC is even able to improve rotor speed regulation with reduced blade pitch actuation.
- In addition, the proposed IPC is capable of reducing blade out-of-plane displacement, tower fore-aft displacement and platform pitch rotation.

In future works, the authors are working on estimating the reduction of long-term fatigue loads on the pitch actuators. Also, the application of robust NMPC for systems with

Parameter	Baseline		NMPC		Reduction (%)	
	LC #1	LC #2	LC #1	LC #2	LC #1	LC #2
Rotor speed (rpm)	0.816	0.770	0.824	0.620	-0.98	19.48
Platform pitch (deg)	1.102	1.154	0.893	0.838	18.95	27.38
Platform roll (deg)	0.167	0.131	0.158	0.120	5.38	8.39
Blade pitch angle (deg)	3.271	2.248	3.042	1.956	7.00	12.99
Blade out-of-plane(m)	1.127	0.964	1.069	0.859	5.14	10.89
Blade in-plane (m)	0.395	0.410	0.394	0.405	0.25	1.22
Tower fore-aft (m)	0.101	0.099	0.090	0.082	10.89	17.17
Tower side-to-side (m)	0.019	0.014	0.020	0.014	-5.2	0.00

Table 1. Standard deviation of the responses

model and/or measurement uncertainties are also being investigated.

Appendix A. EQUATIONS OF MOTION OF THE REDUCED ORDER MODEL

The linearized equations of motion of the six degree of freedom system excluding the actuator models (see equation 3) is presented in this section. To derive the equations of motion, first it is assumed that the wind turbine is rotating at a constant speed. The generator speed error degree of freedom is decoupled from the rest of the system. This approach is undertaken since the inclusion of the generator speed error as a degree of freedom introduces non-linearities in the form of cosine and sine terms which cannot be linearized using small angle approximation. The generator speed error degree of freedom is described as

$$\dot{q}_\varepsilon = \delta\Omega = \Omega_0 - q_{GeAz}$$
$$q_\varepsilon = \int_0^t \dot{q}_\varepsilon dt = \int_0^t (\Omega_0 - q_{GeAz})dt \qquad (A.1)$$
$$\ddot{q}_\varepsilon = \delta\dot{\Omega} = \ddot{q}_{GeAz}$$

Where, Ω_0 is the rated rated rotor speed of the FOWT. The equation of motion of this degree of freedom assuming only intergal action K_I can be obtained from Jonkman (2007) as

$$I_{DT}\ddot{q}_\varepsilon + \left(-\frac{P_0}{\Omega_0^2}\right)\dot{q}_\varepsilon + \frac{1}{\Omega_0}\left(-\frac{\partial P_0}{\partial \theta}\right)N_{Gear}K_I q_\varepsilon = 0 \quad (A.2)$$

Where, $I_{DT} = I_{Rotor} + N_{Gear}^2 I_{Gen}$ is the drive-train intertia cast into the low speed shaft, I_{Rotor} is the inertia of the rotor, I_{Gen} is the inertia of the generator relative to the high speed shaft, N_{Gear} is the gear box ratio. P_0 is the rated mechanical power. As recommended by Jonkman (2010) the integral gain K_I is selected such that the frequency of this degree of freedom is 0.2 rad/s. Therefore, the stiffness term can be written as

$$\frac{1}{\Omega_0}\left(-\frac{\partial P_0}{\partial \theta}\right)N_{Gear}K_I = 0.2^2 I_{DT} = k_{\varepsilon\varepsilon} \qquad (A.3)$$

The mass, stiffness and damping matrix of the linearized six degree of freedom system are obtained as

$$\mathbf{M} = \begin{bmatrix} m_{PP} & m_{PT} & m_{PB1} & m_{PB2} & m_{PB3} & 0 \\ & m_{TT} & m_{TB1} & m_{TB2} & m_{TB3} & 0 \\ & & m_{BB} & 0 & 0 & 0 \\ & & & m_{BB} & 0 & 0 \\ & sym & & & m_{BB} & 0 \\ & & & & 0 & I_{DT} \end{bmatrix} \qquad (A.4)$$

$$\mathbf{C} = \begin{bmatrix} c_{PP} & 0 & 0 & 0 & 0 & 0 \\ & c_{TT} & 0 & 0 & 0 & 0 \\ & & c_{BB} & 0 & 0 & 0 \\ & & & c_{BB} & 0 & 0 \\ & sym & & & c_{BB} & 0 \\ & & & & & \left(-\frac{P_0}{\Omega_0^2}\right) \end{bmatrix} \qquad (A.5)$$

$$\mathbf{K} = \begin{bmatrix} k_{PP} & 0 & 0 & 0 & 0 & 0 \\ & k_{TT} & 0 & 0 & 0 & 0 \\ & & k_{BB}^1 & 0 & 0 & 0 \\ & & & k_{BB}^2 & 0 & 0 \\ & sym & & & k_{BB}^3 & 0 \\ & & & & & 0 & k_{\varepsilon\varepsilon} \end{bmatrix} \qquad (A.6)$$

where sym stands for symmetric and denotes that the above matrices are symmetric. The quantities in the above matrices can be given as

$$m_{PP} = 12H_t^2\int_0^L m_b(r)\mathrm{d}r + \sum_{i=1}^3\left[4H_t\int_0^L rm_b(r)\mathrm{d}r\cos(\psi_i)\right.$$
$$\left. + \int_0^L r^2 m_b(r)\mathrm{d}r\cos^2(\psi_i)\right] + \int_0^{H_t} hm_t(h)\mathrm{d}h$$
$$+ H_t^2 m_{NH} + I_P + I_P^{AM}$$
$$(A.7)$$

$$m_{PT} = 6H_t\int_0^L m_b(r)\mathrm{d}r + \int_0^{H_t} hm_t(h)\phi_t(h)\mathrm{d}h \quad (A.8)$$

$$m_{PBi} = 2H_t\int_0^L \phi_b(r)m_b(r)\mathrm{d}r$$
$$+ \int_0^L r\phi_b(r)m_b(r)\mathrm{d}r\cos(\psi_i) \qquad \text{for } i = 1 \text{ to } 3$$
$$(A.9)$$

$$m_{TB} = \int_0^L \phi_b(r)m_b(r)\mathrm{d}r \qquad (A.10)$$

$$m_{TT} = 3\int_0^L m_b(r)\mathrm{d}r + \int_0^{H_t} \phi_t^2 m_t(h)\mathrm{d}h + m_{NH} \quad (A.11)$$

Where, H_t is the height of the tower and L is the length of the blades. $m_b(r)$ and $m_t(h)$ are mass per unit length of the blades and tower respectively. ψ_i is the azimuth angle of the ith blade. m_{NH} is the combined mass of the nacelle and hub. I_P is the rotational inertia of

the platform and I_P^{AM} is the hydrodynamic added mass coefficient associated with the platform pitch degree of freedom. $\phi_b(r)$ and $\phi_t(h)$ are the normalized fundamental model shapes of the blades and tower respectively. c_{PP} is the linear hydrodynamic damping coefficient associated with the platform pitch degree of freedom, c_{TT} and c_{BB} are structural damping coefficient of the tower and the blades respectively. k_{PP} is the summation of hydro-static and mooring lines stiffness associated with the platform pitch degree of freedom. k_{TT} is the elastic stiffness of the tower and $k_{BB}^i = k_{BB}^e + k_{BB}^c + k_{BB}^g \cos(\psi_i)$ is the summation of the elastic stiffness k_{BB}^e centrifugal stiffness k_{BB}^c and gravitational stiffening/softening of the ith blade. More details on these terms can be found in (Sarkar and Chakraborty, 2019).

REFERENCES

Bossanyi, E. (2003). Individual blade pitch control for load reduction. *Wind energy*, 6(2), 119–128.

Bossanyi, E. (2005). Further load reductions with individual pitch control. *Wind energy*, 8(4), 481–485.

Bossanyi, E.A., Fleming, P.A., and Wright, A.D. (2013). Validation of individual pitch control by field tests on two-and three-bladed wind turbines. *IEEE Transactions on Control Systems Technology*, 21(4), 1067–1078.

Burton, T., Jenkins, N., Sharpe, D., and Bossanyi, E. (2011). *Wind energy handbook*. John Wiley & Sons.

Fitzgerald, B., Sarkar, S., and Staino, A. (2018). Improved reliability of wind turbine towers with active tuned mass dampers (atmds). *Journal of Sound and Vibration*, 419, 103–122.

Henriksen, L.C. (2011). *Model predictive control of wind turbines*. Technical University of Denmark (DTU).

Jonkman, B.J. (2009). Turbsim user's guide: Version 1.50. Technical report, National Renewable Energy Lab.(NREL), Golden, CO (United States).

Jonkman, J.M. (2007). *Dynamics modeling and loads analysis of an offshore floating wind turbine*. University of Colorado at Boulder.

Jonkman, J.M. (2010). *Definition of the Floating System for Phase IV of OC3*. Citeseer.

Jonkman, J.M. and Buhl Jr, M.L. (2005). Fast user's guide-updated august 2005. Technical report, National Renewable Energy Laboratory (NREL), Golden, CO.

Koerber, A. and King, R. (2013). Combined feedback–feedforward control of wind turbines using state-constrained model predictive control. *IEEE Transactions on Control Systems Technology*, 21(4), 1117–1128.

Lindelöw, P. (2008). *Fiber Based Coherent Lidars for Remote Wind Sensing Ph. D.* Ph.D. thesis, thesis, Danish Technical University, Copenhagen, Denmark.

MATLAB (2018). *version 9.4.0 (R2018a)*. The Math-Works Inc., Natick, Massachusetts.

Mirzaei, M., Soltani, M., Poulsen, N.K., and Niemann, H.H. (2013). An mpc approach to individual pitch control of wind turbines using uncertain lidar measurements. In *Control Conference (ECC), 2013 European*, 490–495. IEEE.

Mughal, M.H. and Guojie, L. (2015). Review of pitch control for variable speed wind turbine. In *2015 IEEE 12th Intl Conf on Ubiquitous Intelligence and Computing and 2015 IEEE 12th Intl Conf on Autonomic and Trusted Computing and 2015 IEEE 15th Intl Conf on Scalable Computing and Communications and Its Associated Workshops (UIC-ATC-ScalCom)*, 738–744. IEEE.

Namik, H. and Stol, K. (2010). Individual blade pitch control of floating offshore wind turbines. *Wind Energy: An International Journal for Progress and Applications in Wind Power Conversion Technology*, 13(1), 74–85.

Namik, H. and Stol, K. (2011). Performance analysis of individual blade pitch control of offshore wind turbines on two floating platforms. *Mechatronics*, 21(4), 691–703.

Namik, H. and Stol, K. (2014). Individual blade pitch control of a spar-buoy floating wind turbine. *system*, 1(3), 6.

Odgaard, P.F., Larsen, L.F., Wisniewski, R., and Hovgaard, T.G. (2016). On using pareto optimality to tune a linear model predictive controller for wind turbines. *Renewable Energy*, 87, 884–891.

Pierson Jr, W.J. and Moskowitz, L. (1964). A proposed spectral form for fully developed wind seas based on the similarity theory of sa kitaigorodskii. *Journal of geophysical research*, 69(24), 5181–5190.

Raach, S., Schlipf, D., Sandner, F., Matha, D., and Cheng, P.W. (2014). Nonlinear model predictive control of floating wind turbines with individual pitch control. In *2014 American Control Conference*, 4434–4439. IEEE.

Sarkar, S. and Chakraborty, A. (2018). Optimal design of semiactive mr-tlcd for along-wind vibration control of horizontal axis wind turbine tower. *Structural Control and Health Monitoring*, 25(2).

Sarkar, S. and Chakraborty, A. (2019). Development of semi-active vibration control strategy for horizontal axis wind turbine tower using multiple magneto-rheological tuned liquid column dampers. *Journal of Sound and Vibration*, 457, 15–36.

Sarkar, S. and Fitzgerald, B. (2019). Vibration control of spar-type floating offshorewind turbine towers using a tuned mass-damper-inerter. *Structural Control and Health Monitoring*, e2471. doi: https://doi.org/10.1002/stc.2471.

Sarkar, S., Fitzgerald, B., and Basu, B. (2020). Individual blade pitch control of floating offshore wind turbines for load mitigation and power regulation. *IEEE Transactions on Control Systems Technology*. doi: 10.1109/TCST.2020.2975148.

Schlipf, D., Grau, P., Raach, S., Duraiski, R., Trierweiler, J., and Cheng, P.W. (2014). Comparison of linear and nonlinear model predictive control of wind turbines using lidar. In *2014 American Control Conference*, 3742–3747. IEEE.

Schlipf, D., Schlipf, D.J., and Kühn, M. (2013). Nonlinear model predictive control of wind turbines using lidar. *Wind energy*, 16(7), 1107–1129.

Soliman, M., Malik, O., and Westwick, D. (2010). Multiple model mimo predictive control for variable speed variable pitch wind turbines. In *Proceedings of the 2010 American Control Conference*, 2778–2784. IEEE.

Valpy, B., Hundleby, G., Freeman, K., Roberts, A., and Logan, A. (2017). *InnoEnergy - Future renewable energy costs: Offshore wind*. BVG Associates.